

RESEARCH ARTICLE

Innovative approach to solar hydrogen generation using SnO₂ photocatalyst in water splitting

Muhammad Junaid¹  | Mohamed Sharaf² | Mohammed EI-Meligy^{3,4} |
 Muhammad Amjad Riaz⁵ | Mohd Arif Dar⁶ | Irfan Ullah Khan⁷

¹Institute of Physics, The Islamia University of Bahawalpur, Bahawalpur, Pakistan

²Department of Industrial Engineering, College of Engineering, King Saud University, Riyadh, Saudi Arabia

³Jadara University Research Center, Jadara University, Irbid, Jordan

⁴Applied Science Research Center, Applied Science Private University, Amman, Jordan

⁵Department of Chemistry, University of Education Lahore, Vehari Campus, Vehari, Pakistan

⁶Faculty of Allied Health Sciences, Chettinad Hospital, and Research Institute, Chettinad Academy of Research and Education, Chennai, India

⁷Department of Integrative Biology, The College of Arts and Sciences, Oklahoma State University, Stillwater, Oklahoma, USA

Correspondence

Muhammad Junaid, Institute of Physics, The Islamia University of Bahawalpur, 63100 Bahawalpur, Pakistan.
 Email: mjunaid310@yahoo.com

Funding information

King Saud University, Grant/Award Number: RSPD2025R704

Abstract

This research explores the capabilities of SnO₂ thin films in renewable energy, with a focus on hydrogen generation through photoelectrochemical (PEC) water splitting. X-ray diffraction (XRD) analysis identifies a tetragonal rutile crystal structure, indicating a highly crystalline phase free from secondary phases. A crystallite size of about 40 nm, determined via the Debye–Scherrer formula, suggests enhanced catalytic suitability for PEC applications. Scanning electron microscopy (SEM) reveals a web-like, rough surface, beneficial for water splitting by providing a high surface area that improves light absorption and charge transfer. The interconnected SnO₂ nanoparticles, averaging 28.63 nm in size, create active sites that further boost photocatalytic performance. UV-Vis spectroscopy shows strong absorption in the UV range (300–330 nm) with limited visible light absorption, consistent with a wide bandgap of approximately 3.63 eV. With 72.5% transparency in the visible spectrum, SnO₂ proves effective as a transparent conducting oxide (TCO), advantageous in optoelectronic devices. Electrochemical impedance spectroscopy (EIS) highlights low charge transfer resistance, and linear sweep voltammetry (LSV) reveals significant photocurrent density, supporting SnO₂'s effectiveness in PEC applications. The solar-to-hydrogen (STH) efficiency is 3.526% at 0.8 V, demonstrating SnO₂'s proficiency in hydrogen production. Additionally, chronoamperometry confirms the film's stability and light responsiveness. A high hydrogen production rate of 3256.93 mol/g over 6 h is attributed to the porous structure of the film, which enhances light harvesting and the hydrogen evolution reaction. These findings establish SnO₂ thin films as a promising material for hydrogen generation and renewable energy applications.

KEYWORDS

CO₂ reduction, green hydrogen, photocatalysis, photo (electro) catalysis, semiconductors, solar water splitting

1 | INTRODUCTION

Tin oxide nanoparticles are tiny particles of the compound tin oxide, which is a wide bandgap semiconductor

material. Tin oxide nanoparticles are of interest in the fields of nanotechnology and materials science due to their unique electronic and optical properties, which make them suitable for use in a variety of applications,

including gas sensing and energy conversion. In gas sensing, tin oxide nanoparticles are used to detect a variety of gases, such as nitrogen oxides and carbon monoxide, by changing their electrical resistance in response to the presence of the gas. This makes tin oxide-based gas sensors highly sensitive and selective compared to other types of gas sensors [1]. In energy conversion, tin oxide nanoparticles are used as photocatalysts in water-splitting reactions, where they can use light to split water molecules into hydrogen and oxygen. This makes tin oxide nanoparticles an important material to produce clean hydrogen fuel. Tin oxide nanoparticles can be synthesized through a variety of methods, including chemical synthesis and physical deposition. They can also be engineered to improve their performance by changing their size, shape, or crystal structure [2]. Overall, tin oxide nanoparticles are a promising material in the fields of nanotechnology and materials science due to their unique electronic and optical properties and their potential for use in gas sensing and energy conversion applications. SnO₂ nanoparticles are inorganic semiconductor nanoparticles made up of tin and oxygen atoms. These nanoparticles have interesting structural, optical, electrical, and photocatalytic properties. Due to their unique properties, tin dioxide nanoparticles have a wide range of applications in various fields, such as gas sensing, electronics, solar cells, and environmental remediation [3].

One of the significant applications of SnO₂ nanoparticles is in gas sensing. SnO₂ nanoparticles have high sensitivity and selectivity toward several gases, making them ideal for gas-sensing applications. Tin dioxide nanoparticles can detect hazardous gases, such as carbon monoxide, methane, and nitrogen dioxide. SnO₂ nanoparticles are also used in electronic applications. They are preferred for electronic devices because of their high electron mobility and high electrical conductivity. Due to their wide bandgap, they are also used as a transparent conductor in solar cells, flat-panel displays, and touch screens. In addition, SnO₂ nanoparticles exhibit excellent photocatalytic activity. They can decompose many organic and inorganic toxic compounds into harmless gas or liquids under UV irradiation. This property makes them useful in the removal of pollutants from wastewater treatment, air purification, and water quality improvement. However, it is important to consider the potential health and environmental hazards when handling SnO₂ nanoparticles. Special precautions and safety measures should be followed to reduce the risks [4].

Mohammed Ali Dheyab et al. [5] in 2022, given the importance of nanotechnology in all branches of science, has emerged as the most promising research field. The fascinating properties of SnO₂ NPs, which have been improved by manufacturing this material in the nanoscale

range, have attracted a lot of interest in recent years. Lithium-ion batteries, solar panels, supercapacitors, photocatalysis, antioxidants, and other fields of study have all demonstrated the efficacy of SnO₂ NPs. This led to a thorough investigation into many synthetic approaches to produce SnO₂ NPs. A few researchers have summarized the SnO₂ NPs, but because they concentrated on the green preparation method, their research was constrained in terms of planning and application. The innovative aspect of the current work is a review of all SnO₂ NPs nanopreparation methods. The techniques used to create SnO₂ NPs include chemical, physical, and biological processes. In comparison to other methods, wet chemical processing is preferable for the large-scale manufacture of uniformly morphologically structured nanomaterials and nanoparticles. Chemical manufacturing of nanomaterials is frequently simple, requiring just ambient temperature process settings, and the end products exhibit higher homogeneity and a smaller size distribution than those produced by other methods. The preparation of green metal oxide nanoparticles is a recent area of research with a focus on it. A thorough investigation should be conducted on this subject at this time considering the significance of this nanomaterial, the diversity of its features, and the diversity of its applications in various sectors [6].

SnO₂ has a bandgap of 3.6 eV, which enables it to absorb UV light effectively. This is essential for its photocatalytic properties, as UV photons can excite electrons from the valence band to the conduction band, generating electron-hole pairs necessary for reactions like hydrogen production. Although SnO₂ cannot absorb much visible light because of its large bandgap, its photocatalytic efficiency can be enhanced by modifying it to utilize natural sunlight more effectively. Regarding charge transport, SnO₂'s high electron mobility and n-type semiconductor characteristics support the efficient movement of electrons, facilitating processes like proton reduction. The material's capacity to separate electron-hole pairs and its relatively low recombination rate further improves its photocatalytic performance. SnO₂ also demonstrates strong stability in photocatalytic applications, with excellent resistance to degradation from UV exposure and chemical corrosion in aqueous environments, making it a durable option for long-term hydrogen production. Furthermore, its resistance to photocorrosion ensures that it maintains efficiency during prolonged photocatalytic processes.

2 | SnO₂ THIN FILM PREPARATION

The process of developing a thin film of SnO₂ on an ITO substrate involved thermal vapor deposition. The starting

material was 0.5 g of 99% pure SnO₂ powder from Sigma-Aldrich, and the tungsten boat was 99.9% pure SnO₂. The working chamber contained a metal wrap with a vacuum system, substance condensation, and vapor deposition. The diffusion pump heater was turned on to warm up the oil, and the tungsten boat containing SnO₂ was electrically heated. The source material was evaporated and deposited on the substrates using thermal energy. After deposition, the baffle valve was closed, the diffusion pump was turned off, and the rotary van pump and backing valve ran for a while. The water supply was then shut off, and the main power was turned off. A very thin film of SnO₂ was deposited on the Borosilicate and ITO substrate [7–9].

3 | XRD STUDY

The XRD spectra for SnO₂ thin films were obtained using a Bruker D8 Advance powder X-ray diffractometer, equipped with Cu K α wavelength $\lambda = 1.5406\text{\AA}$. Diffraction patterns were collected with a step increment of approximately 0.025° and an acquisition time of 18 s per step. To ensure consistent measurements across the samples, rotation was applied during analysis. The D8 Bruker diffractometer was operated at 40 kV and 40 mA, with scans covering a 2 θ range from 0° to 80°. XRD is a technique used to study the crystal structure and phase identification of nanoparticles. It provides information about crystal size, lattice parameters, and preferred orientation. In this study, SnO₂ thin films grown on an ITO substrate were analyzed using PVD techniques. The XRD patterns showed a tetragonal rutile structure, indicating the lattice

parameters $a = b = 4.738\text{\AA}$, $c = 3.187\text{\AA}$ SnO₂ thin films without secondary phases (Figure 1).

$$D = \frac{k \times \lambda}{\beta \cos \theta} \quad (1)$$

The XRD peaks were observed at angle 2 theta 26.6, 33.9, 37.9 and compared with standard card JCPDS 41-1445. The average crystallite size was observed to be 40 nm, according to the Debye–Scherrer formula, indicating a small size, making it suitable for hydrogen generation applications [10, 11].

4 | SEM STUDY

The SEM (Cube II Emcraft South Korea) setup is used to analyze and confirm the amorphous nature of the SnO₂ thin films, revealing non-uniform and crack-free surfaces. The thin films appeared featureless, highlighting their consistent and non-uniform nature [12]. The SEM images of SnO₂ at different scan rates are shown in Figure 2. It is clear from the SEM image that the SnO₂ nanoparticle has a weblike structure due to high agglomerations and has all dimensions in the micro range. The size of the nanoparticle is determined by considering more than 80 number of particles, and the average size of the SnO₂ nanoparticle is found to be 28.63 nm via ImageJ software. The shape and size of the SnO₂ become more irregular while increasing the scan rate due to strong agglomeration. The surface morphology of the sample was observed to be rough; these characteristics of SnO₂ helped the absorption of solar spectra for water splitting to generate hydrogen energy as cited in Figure 2(a–c).

A weblike morphology in SnO₂ thin films is highly beneficial for water splitting, offering a large surface area and interconnected pores that boost photocatalytic performance. This structure enhances light absorption, facilitates charge transport, and provides more active sites for water-splitting reactions. The increased porosity also allows electrolytes to penetrate effectively, improving the interaction with reactive sites and enhancing catalytic efficiency. In photoelectrochemical (PEC) cells, weblike SnO₂ can serve as an effective photoanode. This morphology makes SnO₂ films promising for applications in renewable energy and environmental technology.

5 | UV-VIS SPECTROSCOPY

A Shimadzu UV-2600 Plus UV-Vis-NIR spectrophotometer, fitted with an integrating sphere, was employed to evaluate the optical absorption and transmission of films

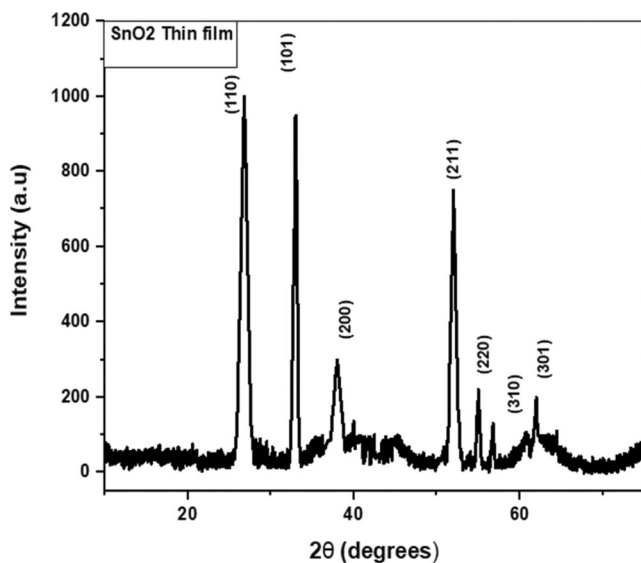


FIGURE 1 XRD analysis of SnO₂.

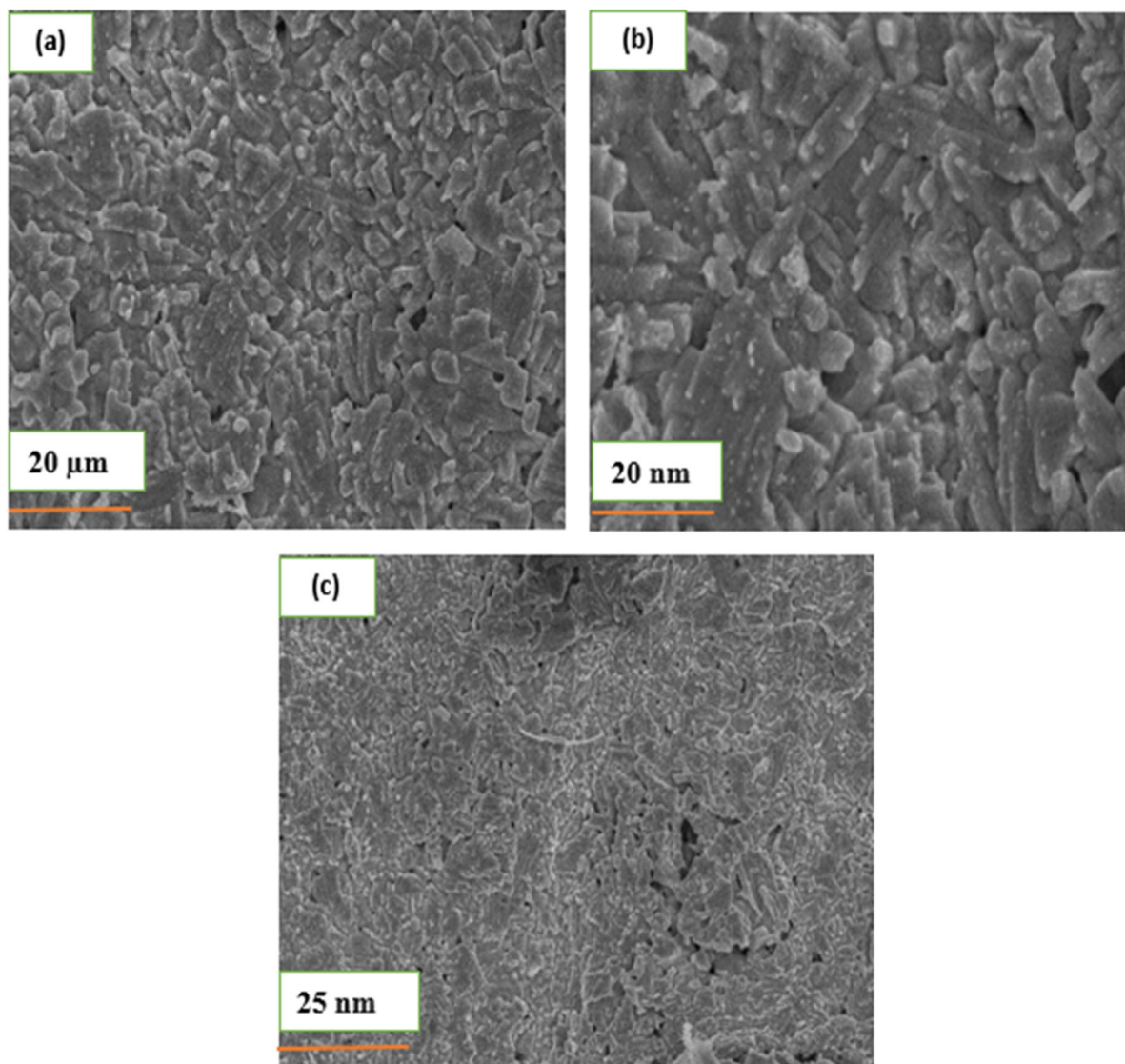


FIGURE 2 (a–c): SEM study of SnO₂ at different scan rates.

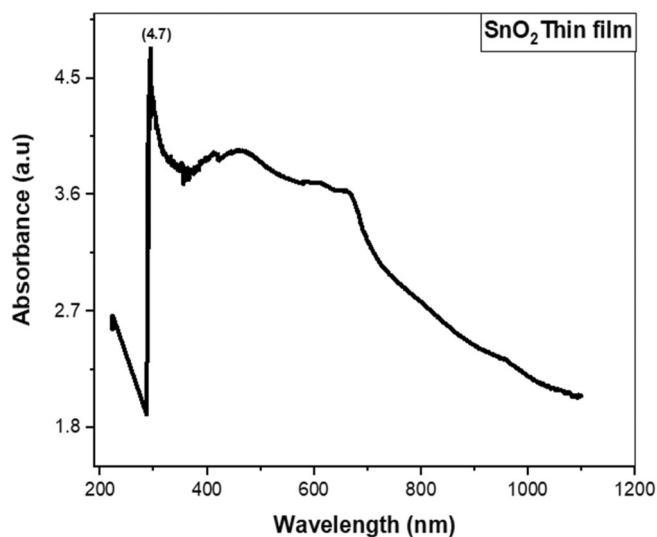


FIGURE 3 UV-Vis analysis of SnO₂.

deposited on quartz substrates. To investigate the optical characteristics of semiconducting materials, useful techniques like UV-visible diffuse reflectance and absorbance spectroscopy are frequently employed. As shown in Figure 3, the reflectance and absorbance spectra of the SnO₂ thin film were examined at various wavelengths ranging from 200 to 800 nm, and the absorption spectrum of SnO₂ typically shows a sharp increase in absorbance in the UV region (around 300–330 nm), corresponding to electron transitions from the valence band to the conduction band. In the range of 300 nm, the thin film showed rapid absorption of 4.7 a.u., which is an excellent sign to absorb UV light, and SnO₂ exhibits minimal absorption in the visible spectrum due to its large bandgap, making it useful as a transparent conducting oxide; they exhibit relatively low absorbance when the wavelength increases [13, 14].

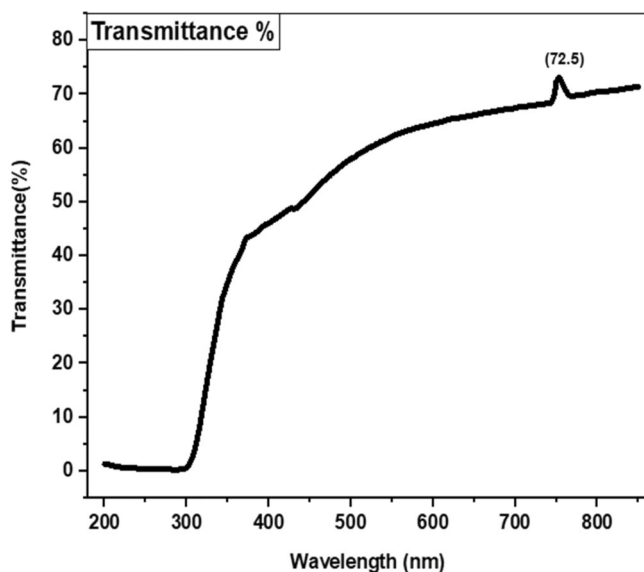


FIGURE 4 Transmittance of SnO₂.

SnO₂'s UV absorption makes it a promising material for UV-driven photocatalytic applications, although its activity can be extended into the visible range through coupling with other materials like other metal oxides. Additionally, SnO₂'s high UV transparency and conductivity make it suitable for use as transparent electrodes in optoelectronic devices such as solar cells and displays. Overall, UV-Vis spectroscopy of SnO₂ offers valuable insights into its bandgap and optical properties, which are critical for its applications in photocatalysis.

SnO₂ thin films are highly transparent in the visible spectrum, making them ideal for applications such as transparent conductive electrodes and optoelectronic devices. However, due to its wide bandgap (3.6 eV), SnO₂ absorbs strongly in the UV range. The transmittance of SnO₂ films is influenced by factors such as film thickness, surface morphology. Thicker films tend to have lower transmittance, while rough and porous surfaces can scatter light, reducing transparency. SnO₂ shows high transmittance in the visible range (above 70%) but absorbs in the UV range (below 380 nm) as reported in Figure 4. This combination of properties makes SnO₂ suitable for transparent conductive oxide applications in devices like solar cells and displays, as well as for photocatalysis in UV-driven reactions. [15].

The data indicates that the thin film possesses high transparency, with a transparency value of 72.5% in the visible region. This high level of transparency suggests that the film exhibits excellent optical quality, and it also indicates minimal absorption losses.

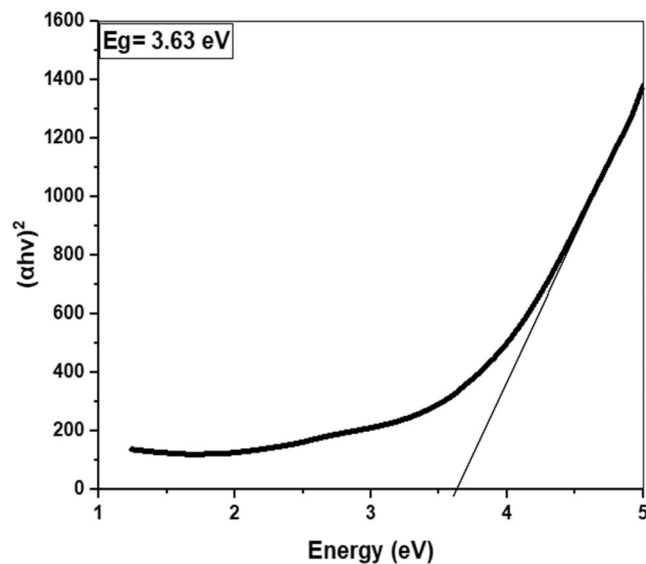


FIGURE 5 Tauc plot of SnO₂.

6 | BANDGAP DETERMINATION

The optical bandgap of the sample deposited on ITO was calculated using a Tauc plot derived from diffuse reflection data and applying the K-M function, as illustrated in Figure 5.

The following expression was used to analyze the optical absorption edge:

$$\alpha = 1/d \ln(1/T) \quad (2)$$

In this equation, d represents film thickness, while T denotes its transmittance. The absorption coefficient (α) depends on the photon energy absorbed strongly by the thin films. To measure the bandgap of the metal oxide semiconductors, the widely used Tauc relation is applied:

$$(\alpha h\nu) = \beta (h\nu - E_g)^n \quad (3)$$

The absorption coefficient α , Planck's constant h , photon frequency (ν), and incident photon energy ($h\nu$) [16]. The β and n factors depend on the likelihood of a transition occurring and the transition from the valence band to the conduction band occurs without a change in momentum, which is important for electronic and optical properties. Since SnO₂ is a direct bandgap semiconductor. Tauc's plot of $(\alpha h\nu)^2$ as a function of $h\nu$ for SnO₂ thin films is shown in Figure 5 [17].

By analyzing the Tauc plot, extract information about the electronic structure and optical properties of SnO₂, which is important for various applications, such as transparent conductive oxides, photocatalysis, and

optoelectronics. The energy bandgap of SnO_2 was found to be 3.63 eV [9].

7 | ELECTROCHEMICAL ANALYSIS

When preparing an electrolyte for a cyclic voltammetry experiment, it is important to specify the exact composition. To study hydrogen evolution, a common electrolyte 1 M KOH is used. The pH of the electrolyte should also be reported, as it can affect the electrochemical processes, such as the hydrogen evolution reaction. Additionally, the temperature at which the measurements are taken should be 30°C , as temperature can influence the reaction kinetics and impedance, with common settings being 30°C .

7.1 | EIS study

Electrochemical impedance spectroscopy (EIS) measurements were performed in the dark using a potentiostat (Autolab, PGSTAT-30) equipped with a frequency analyzer. In this plot, the semicircle indicates charge transfer resistance, while the low-frequency region reflects diffusion or conductivity. Key parameters analyzed include resistance, capacitance, and charge transfer resistance. High-frequency data gives insight into the resistance of the electrolyte or the film, while the middle frequency range provides information about charge transfer resistance, and the low-frequency data relates to the Warburg impedance, which reflects ion or charge carrier diffusion. A lower charge transfer resistance typically indicates better device efficiency. Overall, EIS provides crucial information on the charge transfer, resistance, and capacitance of SnO_2 , helping optimize its performance in different applications and contributing to the development of more efficient devices.

It provided information on the charge-transfer resistance and properties of different counter electrodes at the electrode/electrolyte interface, and EIS analysis was conducted on symmetric cells containing two identical electrodes [18]. The charge-transfer resistance of SnO_2 was found to be lower than that of another semiconductor. The electrochemical performance of the thin film was observed through cyclic voltammetry and chronoamperometry. The EIS analysis revealed semicircles in the Nyquist plots, representing the charge-transfer processes at both the CE/electrolyte interface and the electrolyte interface, respectively. The low impedance curve observed for the SnO_2 -based cell indicates efficient charge transfer from the electrolyte interface to the

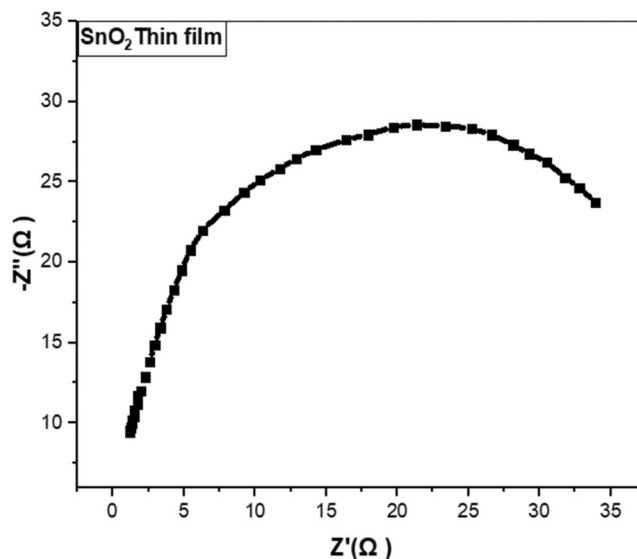


FIGURE 6 Nyquist plot of SnO_2 .

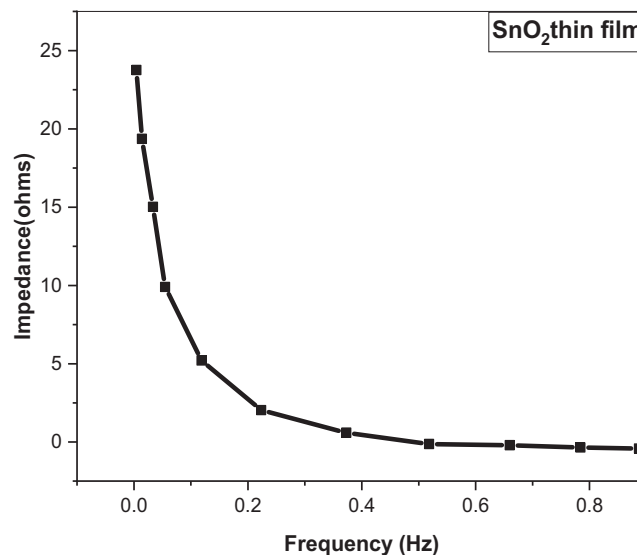


FIGURE 7 Bode plot of SnO_2 thin film.

working electrode [19]. This suggests that SnO_2 demonstrates excellent charge-transfer characteristics, leading to maximum photocurrent generation under suitable wavelengths within the solar spectra. The SnO_2 thin film was quite better for use as an electrode in energy storage devices due to its improved electrochemical performance. It is attributed to increased surface area and improved charge transfer kinetics as reported in Figure 6.

7.2 | Bode plot

The Nyquist plot of SnO_2 thin films shows how the electrochemical impedance varies with frequency, which is

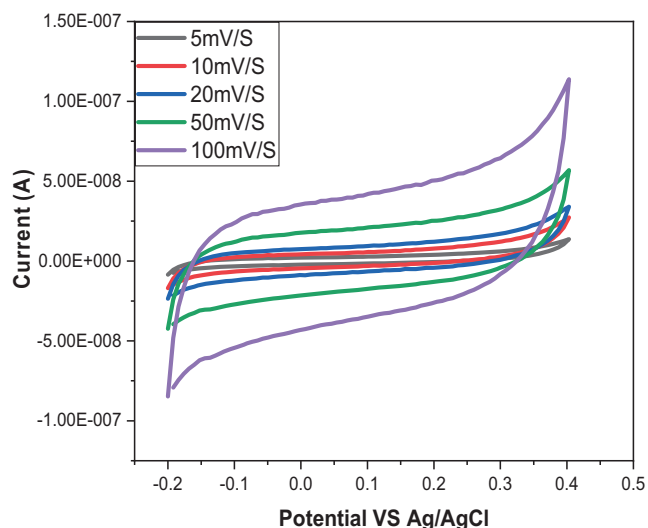


FIGURE 8 ECSA analysis of SnO₂.

crucial for understanding the material's electrochemical behavior in applications such as energy storage devices, sensors, and electrocatalysis. At low frequencies, the behavior of SnO₂ thin films is dominated by diffusion-controlled processes, often described by Warburg impedance (Z_W). This is seen as a straight line with a 45-degree slope in the Nyquist plot, which represents the diffusion of ions in and out of the SnO₂ film and the electrolyte, as reported in Figure 7.

As the frequency decreases further, the plot typically shows a longer tail, extending vertically toward the real axis. This behavior corresponds to diffusion limitations, as ions have slower movement at low frequencies. The steepness of this line is related to the diffusion coefficient and the ability of ions to move through the SnO₂ thin film and the electrolyte.

7.3 | Electrochemical active surface area (ECSA)

ECSA is an important parameter used to characterize the activity of a material in electrochemical reactions. It refers to the surface area that is actively involved in electrochemical reactions, such as those occurring in electrocatalysis.

SnO₂ is a semiconductor with a wide bandgap, known for its excellent conductivity, stability, and large surface area, making it a popular choice as an electrode material. ECSA represents the surface area of SnO₂ that is electrochemically active, meaning the surface area that participates in charge transfer processes, such as during the hydrogen evolution reaction (HER) or other redox reactions. To evaluate the ECSA of SnO₂, techniques such as

CV is used. These methods help in measuring important parameters like current response, charge transfer resistance, which are linked to the material's active surface area. The ECSA of SnO₂ can be influenced by factors such as particle size, surface structure, hydration, and temperature, with nanostructured SnO₂ typically showing a higher ECSA due to a larger surface area. Modifying SnO₂ with other materials can also enhance its electrochemical properties. The high ECSA of SnO₂ makes it a better material for applications in electrocatalysis. Ultimately ECSA is crucial for optimizing SnO₂'s performance in electrochemical applications as cited in Figure 8.

The ECSA can be calculated by the equation below:

$$\text{ECSA} = Q/C_H \quad (4)$$

Q is the total charge from CV experiments, while C_H is the charge required to absorb one monolayer of hydrogen per unit area. This value is 210 $\mu\text{C}\cdot\text{cm}^{-2}$ for SnO₂. The electrochemical charge related to a known redox process can be used to calculate the ECSA. For instance, the charge in a cyclic voltammetry scan can be correlated with the number of active sites involved in the electrochemical reaction. From the CV curve, the ECSA is calculated to be 6 cm^2 . Thin films of SnO₂ have a lower ECSA compared to nanoparticulate forms because their surface area is confined to the thin, exposed surface of the film, which is relatively smooth and compact. Nanoparticles, with their larger surface area and higher degree of roughness and porosity, provide more electrochemically active sites and allow for better accessibility to the electrolyte. Therefore, in applications like catalysis or energy storage, nanoparticulate SnO₂ generally offers a higher ECSA, leading to enhanced electrochemical performance.

7.4 | LSV measurements

Linear sweep voltammetry measurements (LSV) were performed in the dark using an Autolab Potentiostat (PGSTAT-30) equipped with a frequency analyzer. LSV of SnO₂ offers valuable insights into its electrochemical characteristics, including onset potential, current density, and stability. This method is particularly beneficial for evaluating SnO₂'s performance in photoelectrochemical cells, gas sensors, and energy storage systems. By analyzing these parameters, LSV helps assess the material's efficiency and behavior under different electrochemical conditions, which is essential for optimizing its use in various technological applications.

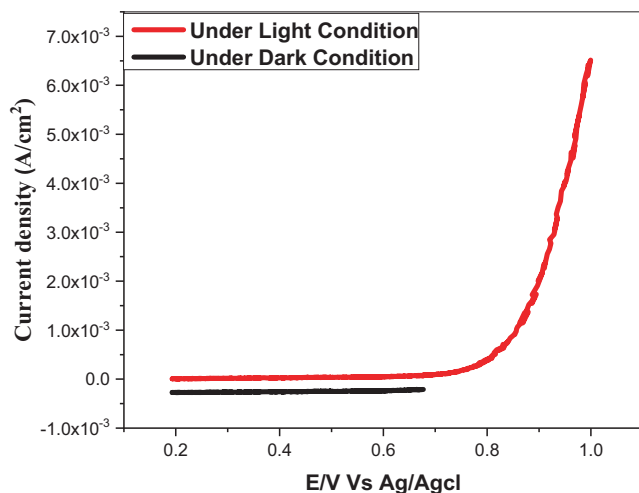


FIGURE 9 LSV measurements of SnO₂.

The STH% of SnO₂ thin film was calculated using the formula below:

$$\text{STH}\% = \frac{(1.23 - V_{\text{bias}})J}{P} \times 100\% \quad (5)$$

where V_{bias} represents the applied voltage using solar spectra between the working and reference electrodes (AgCl/Ag). J denotes the photocurrent density generated by the SnO₂ thin film [20, 21]. P is the solar intensity at the Earth's surface, which is typically 1000 W/m². Upon experimental measurement, the STH% of the SnO₂ thin film was found to be 3.526% at an applied voltage of 0.8 V as mentioned in Figure 9.

To further understand the change in photocurrent under different conditions, the following formula was utilized:

$$J = J_{\text{light}} - J_{\text{dark}} \quad (6)$$

In this context: J_{light} represents the photocurrent density measured under light conditions. J_{dark} represents the photocurrent density measured under dark conditions. [20, 21] The applied voltage range is 0.1 to 1 V but the reported voltage is 0.8v. The total irradiance is 1000 W/m² at sea level under clear sky conditions. Approximately 6 h of exposure to the light source is 21.6 MJ/m². This photocurrent of SnO₂ yields a significantly higher current at low voltage.

7.5 | Chronoamperometry analysis

Autolab Potentiostat (PGSTAT-30) equipped with a frequency analyzer was used for the chronoamperometry

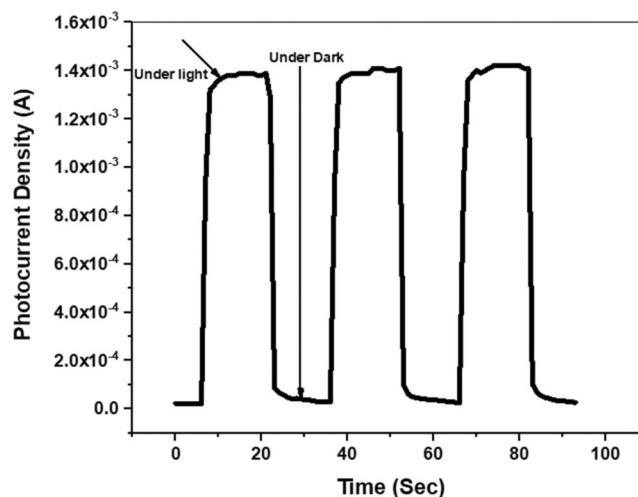


FIGURE 10 Chronoamperometry under dark/light.

analysis. Chronoamperometry steps the working electrode's voltage and monitors the resultant current from faradaic processes as a function of time. After applying a single or double potential step to the electrochemical system's working electrode, current response and time are measured. The peak oxidation current/peak reduction current ratio provides little information about electrolyzed compounds. Here in our case, a fixed voltage value of 0.44 V versus Ag/AgCl was used. On-off irradiation cycles were used to study how materials react to light. Applying the same oxidation potential of 0.44 V and with lamp on-off irradiation of 10 s to measure the value of transient current as cited in Figure 10. The results of the chronoamperometry show that the current in the samples significantly increased after being exposed to light. The findings indicate that SnO₂ is steady and stable for the necessary characteristics of a photoanode [21].

Chronoamperometric analysis of SnO₂ provides essential information on charge transfer kinetics, electrochemical stability, and the material's response to various electrochemical conditions. This technique is particularly useful for evaluating the performance of SnO₂ in applications such as gas sensing, photoelectrochemical cells, and energy storage devices, contributing to the optimization of SnO₂ for these technologies.

7.6 | Hydrogen generation measurement

Photoelectrochemical water splitting is a promising method for producing hydrogen, and its efficiency is significantly influenced by the characteristics of the light source. The UV-Vis range typically spans from 200 to 500 nm, with light intensity varying between 10 and 100 mW/cm². Irradiance levels can range from 100 to

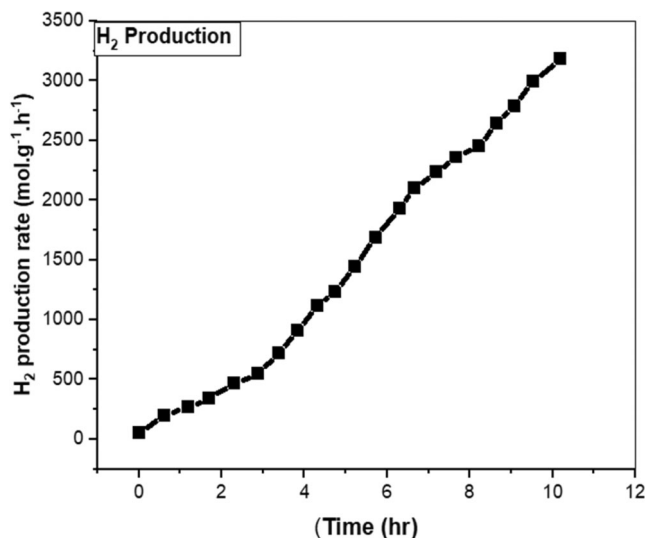


FIGURE 11 Hydrogen evolution of SnO₂.

1000 W/m², depending on the experimental setup. Several light sources are commonly used in PEC water splitting studies, including xenon lamps, LED arrays (such as UV, blue, or white LEDs), solar simulators, and laser sources (e.g., those emitting at 365 or 405 nm). These light sources play a critical role in driving the photocatalytic reactions essential for efficient hydrogen production [22].

SnO₂ is classified as an n-type semiconductor, which means it has an excess of free electrons that enable electrical conductivity. This n-type characteristic results from the presence of oxygen vacancies or the doping of SnO₂ with elements that add extra electrons to the conduction band, increasing its electron density. These free electrons serve as charge carriers, facilitating the movement of current when an electric field is applied. As a result, SnO₂ is commonly used in applications like gas sensors, transparent conductive films, and photocatalysis [23].

Figure 11 illustrates the rate of hydrogen production from the SnO₂ thin film. SnO₂ has been found to create hydrogen more quickly than other semiconductor materials. The enhanced rate of hydrogen synthesis is due to the thin film's remarkable solar light harvesting capabilities, as shown by multiple tests such as absorbance, electrochemical impedance spectroscopy, and LSV [24]. Scanning electron microscopy research revealed that the porosity of the SnO₂ thin film plays a major role in the extraordinary rate of hydrogen production. Porosity contributes to the overall rise in the rate of hydrogen generation by facilitating effective hydrogen evolution processes [25–31].

In 6 h, the average rate of hydrogen production was determined to be 3256.93 mol / g⁻¹. This noteworthy rate emphasizes the potential of SnO₂ as a viable contender

for hydrogen evolution and applications involving renewable energy.

8 | CONCLUSION

The SnO₂ thin films show strong potential for renewable energy applications, especially in hydrogen production via PEC water splitting. XRD analysis confirms that the SnO₂ films have a well-defined tetragonal rutile structure, with lattice parameters $a = b = 4.738 \text{ \AA}$, $a = b = 4.738 \text{ \AA}$, $a = b = 4.738 \text{ \AA}$ and $c = 3.187 \text{ \AA}$, $c = 3.187 \text{ \AA}$, $c = 3.187 \text{ \AA}$, indicating a highly crystalline phase without any secondary phases. The calculated crystallite size of 40 nm, obtained using the Debye–Scherrer formula, makes SnO₂ particularly suitable for catalytic processes in PEC cells. SEM reveals a rough, web-like morphology, which enhances water splitting by providing a large surface area, increasing light absorption, and promoting efficient charge transport. The interconnected SnO₂ nanoparticles, with an average size of 28.63 nm, contribute to the formation of active sites crucial for photocatalytic efficiency. UV-Vis spectroscopy results show that SnO₂ thin films have strong UV absorption (300–330 nm) and minimal visible light absorption due to their wide bandgap of approximately 3.63 eV. This property makes SnO₂ a valuable transparent conducting oxide (TCO) for optoelectronic devices, with a high transparency of 72.5% in the visible spectrum due to its high optical quality and low absorption losses. The bandgap, as analyzed through a Tauc plot, is instrumental in tailoring the optical and electronic features of SnO₂, maximizing its performance in applications such as photocatalysis, gas sensing, and solar cell electrodes. EIS results reveal low charge transfer resistance and impedance, both critical for optimal PEC performance. ECSA of SnO₂, which characterizes the material's electrochemical activity, can be calculated and found to be 6 cm². LSV measurements indicate a high photocurrent density, underscoring the effectiveness of SnO₂ in PEC systems. Additionally, the solar-to-hydrogen (STH) efficiency is calculated at 3.526% under an applied voltage of 0.8 V, demonstrating SnO₂'s efficiency in hydrogen generation. Chronoamperometry results confirm the film's stability and its sensitivity to light, key attributes for an effective photoanode. Hydrogen production measurements indicate a generation rate of 3256.93 mol/g over 6 h, a high yield attributed to SnO₂'s porous structure, which optimizes light capture and enhances the hydrogen evolution reaction. Together, these structural, optical, and electrochemical properties establish SnO₂ thin films as a promising material for hydrogen production and other renewable energy applications.

ACKNOWLEDGMENTS

The authors extend their appreciation to King Saud University, Saudi Arabia, for funding this work through Researchers Supporting Project number (RSPD2025R704), King Saud University, Riyadh, Saudi Arabia.

CONFLICT OF INTEREST STATEMENT

Authors do not have any conflict of interest.

DATA AVAILABILITY STATEMENT

Data will be available on demand from authors.

ORCID

Muhammad Junaid  <https://orcid.org/0000-0001-8641-2185>

REFERENCES

- [1] W. Gu, D. Lu, K. K. Kondamareddy, J. Li, P. Cheng, W. Ho, Y. Wang, Z. Zhao, Z. Wang, *Mater. Today Phys.* **2024**, *46*, 101487.
- [2] Z. Wang, D. Lu, K. K. Kondamareddy, Y. He, W. Gu, J. Li, H. Fan, H. Wang, W. Ho, *ACS Appl. Mater. Interfaces* **2024**, *16*, 48895.
- [3] Y. Xie, J. Dong, Y. Li, X. Ma, N. Wang, X. Meng, Y. Huang, *Acta Mater.* **2025**, *286*, 120706.
- [4] N. Gao, Y. Zeng, J. Wang, D. Wu, C. Zhang, Q. Song, J. Qian, S. Jin, *China Commun.* **2021**, *18*, 253.
- [5] H. Rinnert, P. Miska, M. Vergnat, G. Schmerber, S. Colis, *Appl. Phys. Lett.* **2012**, *100*, 101908.
- [6] S. Tai, C. Bu, Y. Wang, T. Yue, H. Liu, L. Wang, *Chin. J. Aeronaut.* **2024**, *37*, 261.
- [7] W. Fan, Q. Xin, Y. Dai, Y. Chen, S. Liu, X. Zhang, Y. Yang, X. Gao, *Sep. Purif. Technol.* **2025**, *353*, 128394.
- [8] Z. Zou, S. Yang, L. Zhao, *Sci. Rep.* **2024**, *14*, 19091.
- [9] D. Mohammed Ali, A. Azlan Abdul, J. Mahmood S, O. Nazila, *Surf. Interfaces* **2022**, *28*, 101677.
- [10] S. N. Kane, A. Mishra, A. K. Dutta, *J. Phys. Conf. Ser.* **2016**, *755*, 011001. <https://doi.org/10.1088/1742-6596/755/1/011001>
- [11] K. M. Wibowo, M. Z. Sahdan, M. T. Asmah, H. Saim, F. Adriyanto, S. Hadi, *IOP Conf. Ser.: Mater. Sci. Eng.* **2017**, *226*, 12180.
- [12] N. Abdullah, N. M. Ismail, D. M. Nuruzzaman, *IOP Conf. Ser. Mater. Sci. Eng.* **2018**, *319*, 1.
- [13] H. B. Wannes, H. Ben Wannes, R. B. Zaghouani, R. Ouertani, A. Araújo, M. J. Mendes, H. Aguas, E. Fortunato, R. Martins, W. Dimassi, *Mater. Sci. Semicond. Process.* **2018**, *74*, 80.
- [14] M. Warnken, K. Lázár, M. Wark, *Phys. Chem. Chem. Phys.* **2021**, *3*, 1870.
- [15] L.-W. Chou, Y.-Y. Lin, A. T. Wu, *Appl. Surf. Sci.* **2023**, *277*, 30.
- [16] M. O. Daricioglu, C. Durucan, A. F. Dericioglu, *Mater. Sci. Eng., B* **2023**, *294*, 116502.
- [17] S. de Monredon, A. Cellot, F. Ribot, C. Sanchez, L. Armelao, L. Gueneau, L. Delattre, *J. Mater. Chem.* **2022**, *12*, 2396.
- [18] S. Gnanam, V. Rajendran, *J. Sol-Gel Sci. Technol.* **2020**, *56*, 128.
- [19] J. Mu, F. Teng, H. Miao, Y. Wang, X. Hu, *Appl. Surf. Sci.* **2020**, *501*, 143974.
- [20] M. d. S. Pereira, F. A. d. S. Lima, C. B. d. Silva, P. d. T. C. Freire, I. F. d. Vasconcelos, *J. Sol-Gel Sci. Technol.* **2017**, *84*, 206.
- [21] M. Warnken, K. Lázár, M. Wark, *Phys. Chem. Chem. Phys.* **2021**, *3*, 1870.
- [22] P.-M. Lee, C.-H. Liao, C.-H. Lin, C.-Y. Liu, *Appl. Surf. Sci.* **2018**, *442*, 398.
- [23] Y. Zhang, J. Zou, Z. He, Y. Zhao, X. Kang, Y. Zhao, Z. Miao, *J. Alloys Compd.* **2021**, *865*, 158597.
- [24] Bathula Babu, B. Talluri, T. R. Gurugubelli, J. Kim, K. Yoo, *Chemosphere* **2022**, *286*, 131577.
- [25] M. Junaid, Noor-ul-Ain, R. Jabeen, S. A. Buzdar, W. Q. Khan, M. Anwar, M. Javed, F. Warsi, *Physica B Condens. Matter.* **2023**, *651*, 414592.
- [26] M. Junaid, K. M. Batoo, S. G. Hussain, W. Q. Khan, S. Hussain, *Results Chem.* **2023**, *6*, 101102.
- [27] M. Junaid, W. Q. K. Noor-ul-Ain, *Int. J. Hydrogen Energy* **2024**, *52*, 199.
- [28] M. Junaid, K. M. Batoo, M. F. Ijaz, B. Zazoum, *Luminescence* **2024**, *39*, e4821.
- [29] M. Junaid, M. S. Noor-ul-Ain, M. El-Meligy, N. Ahmad, *Luminescence* **2024**, *39*, e70020. <https://doi.org/10.1002/bio.70020>
- [30] M. Junaid, M. Sharaf, M. El-Meligy, Muhammad Amjad Riaz, Irfan ullah Khan improved hydrogen evolution efficiency in water splitting with WO₃ thin-film via physical vapor deposition. <https://doi.org/10.1002/JCCS.202500009>
- [31] T. Thomas, M. A. Mathavan, H. H. Jothirajan, H. Y. Z. Somaily, I. S. Yahia, *Opt. Mater. (Amst)*. **2019**, *99*, 109518. <https://doi.org/10.1016/j.optmat.2019.109518>

How to cite this article: M. Junaid, M. Sharaf, M. EI-Meligy, M. A. Riaz, M. A. Dar, I. U. Khan, *J. Chin. Chem. Soc.* **2025**, *1*. <https://doi.org/10.1002/jccs.70009>